Theory of a Charged Bose Gas. I*

SHANG-KENG MA AND CHIA-WEI WOO
Department of Physics and Institute for Radiation Physics & Aerodynamics, University of California, San Diego, La Jolla, California

(Received 20 February 1967)

This is the first of two papers in which the high-density charged Bose gas at zero temperature is treated by two independent and self-contained methods. In this paper, we are concerned with the excitation spectrum of the system. An analysis of the formal and physical aspects of the theory is followed by a simple numerical calculation. We apply the usual field-theoretic formulation for a Bose system. The Green's functions and other response functions, or propagators, are analyzed, emphasizing the role of the dielectric constant. The general features of the excitation spectrum are described. To apply and to further illustrate the formalism, the low-lying levels are numerically determined to the order of $r_s^{3/4}$ in units of ω_{pl} (the next order beyond the Bogoliubov approximation). r_s is the ratio of the average interparticle distance to the Bohr radius and ω_{pl} is the plasma frequency.

I. INTRODUCTION

THE theory of a high-density charged Bose gas was first studied by Foldy[1] in the Bogoliubov approximation, which is the lowest-order approximation in the expansion parameter $r_s^{3/4}$. The next order approximation has been studied by Brueckner[2] and by Lee and Feenberg,[2] who were only concerned with the ground-state energy. Various aspects of the theory have also been studied by other authors.[3]

The long-range force and the Bose-Einstein condensation are the two outstanding features of the charged Bose system. They give rise to divergent terms in the usual perturbation calculation of the ground-state energy. The difficulty was not resolved until Brueckner[2] demonstrated that the divergent terms cancel and the result is well behaved if one handles the perturbation series consistently.

The appearance of canceling divergent terms implies that an understanding of the formal structure and the more qualitative aspects of the theory has been lacking. While the Coulomb force has been studied extensively for an electron gas, and the formal theory of a neutral Bose system has also been investigated,[4,5] the charged Bose system has not received sufficient attention. This paper is devoted to the exploration of the formal structure of the theory in order to demonstrate the physical implications of the long-range Coulomb interaction and the Bose-Einstein condensation. We shall employ the usual field-theory method and focus our attention on the excitation spectrum. The formal and qualitative analysis provides us with a perturbation calculation involving no divergent term at all.

In Sec. II, we introduce the Green's functions, the density and current propagators, the dielectric constant, and other related functions. By analyzing the structure of the diagrams and through the conservation laws, we derive exact relations among the functions and illustrate the role of the dielectric constant. Following the formal analysis, we give, in Sec. III, a qualitative description of the excited states. The excitation spectrum, as a function of the momentum k of the system, is found to have the following features. For k larger than a certain *cutoff momentum*, there is a continuum of energy levels starting from a finite threshold. For k less than the cutoff momentum, there is, in addition, a discrete level below the continuum (see Fig. 8). The relationship between the discrete level and the threshold of the continuum is discussed. The origin of the finite energy gap and the absence of the low-lying transverse excitations is also discussed. In Sec. IV, the perturbation expansion in powers of $r_s^{3/4}$ for the energy of the discrete level is made. The zeroth-order approximation (i.e., the Bogoliubov approximation) and the first-order approximation are studied. The first-order term is then determined by evaluating the relevant diagrams numerically. The formalism enables us to have a simple numerical procedure involving no divergence or ill-defined integrals. Our results are thus exact to the order $r_s^{3/4}$. A few comments are given in Sec. V.

II. FORMAL STRUCTURE OF THE THEORY

In this section, we set up the formalism and derive a few exact relations which display the simple and important physical features of the theory. Some of these exact relations will be the basis for later calculations.

* This research was supported by the Advanced Research Projects Agency and was monitored by the U.S. Army Research Office, Durham, under Contract No. DA-31-124-ARO-D-257; and the Atomic Energy Commission.

[1] L. L. Foldy, Phys. Rev. **124**, 649 (1961).

[2] K. A. Brueckner, Phys. Rev. **156**, 204 (1967); D. K. Lee and E. Feenberg, *ibid.* **137**, A731 (1965).

[3] M. Girardeau and R. Arnowitt, Phys. Rev. **113**, 755 (1959); M. Girardeau, *ibid.* **127**, 1809 (1962); D. Wright, *ibid.* **143**, 91 (1966); B. W. Ninham, Nucl. Phys. (Netherlands) **53**, 685 (1964); W. H. Bassichis and L. Foldy, Phys. Rev. **133**, A935 (1964); W. H. Bassichis, *ibid.* **134**, A543 (1964); J. M. Stephen, Proc. Phys. Soc. (London) **79**, 994 (1962); E. H. Lieb and A. Y. Sakakura, Phys. Rev. **133**, A899 (1964); F. J. Dyson, Brandeis Summer School Lectures, 1966 (unpublished).

[4] N. M. Hugenholtz and D. Pines, Phys. Rev. **116**, 489 (1959).

[5] J. Gavoret and P. Nozieres, Ann. Phys. (N.Y.) **28**, 349 (1964).

A. The Hamiltonian

The Hamiltonian (the free energy) of the charged Bose system in a unit volume is

$$H=\sum_{\mathbf{k}} n_{\mathbf{k}}(\epsilon_k-\mu)+\sum_{\mathbf{k}\neq 0} V_k(\rho_{\mathbf{k}}\rho_{\mathbf{k}}^{\dagger}-n)/2, \quad (2.1)$$

where

$$\epsilon_k=k^2/2m,$$
$$n_{\mathbf{k}}=a_{\mathbf{k}}^{\dagger}a_{\mathbf{k}},$$
$$V_k=4\pi e^2/k^2,$$
$$\rho_{\mathbf{k}}=\sum_{\mathbf{p}} a_{\mathbf{p}}^{\dagger}a_{\mathbf{p}+\mathbf{k}}. \quad (2.2)$$

μ is the chemical potential and n is the total density, which is a fixed constant. The zero-momentum oscillator is treated classically, i.e.,

$$a_0^{\dagger}=a_0=\sqrt{n_0}, \quad (2.3)$$

and n_0 is regarded as a c number. n_0 is determined by the condition that the free energy shall be minimum at the correct value of n_0:

$$(\partial/\partial n_0)\langle H\rangle=0. \quad (2.4)$$

The brackets $\langle\cdots\rangle$ will always denote the ground-state average. The chemical potential μ is determined by

$$-(\partial/\partial\mu)\langle H\rangle=n. \quad (2.5)$$

The total number of particles not in the condensate is denoted by n':

$$n'=n-n_0. \quad (2.6)$$

Writing out a_0 and $a_0^{\dagger}$ explicitly, the density fluctuation $\rho_{\mathbf{k}}$ has the form

$$\rho_{\mathbf{k}}=(\sqrt{n_0})(a_{\mathbf{k}}+a_{-\mathbf{k}}^{\dagger})+\sum_{\mathbf{p}} a_{\mathbf{p}}^{\dagger}a_{\mathbf{p}+\mathbf{k}}. \quad (2.7)$$

Henceforth, the zero-momentum subscript will always be excluded. The current operator $\mathbf{J}_{\mathbf{k}}$ is defined as

$$\mathbf{J}_{\mathbf{k}}=(\mathbf{k}/2m)(\sqrt{n_0})(a_{\mathbf{k}}-a_{-\mathbf{k}}^{\dagger})+m^{-1}\sum_{\mathbf{p}}(\mathbf{p}+\tfrac{1}{2}\mathbf{k})a_{\mathbf{p}}^{\dagger}a_{\mathbf{p}+\mathbf{k}}. \quad (2.8)$$

Substituting (2.7) in (2.1), we see that there are three kinds of interaction terms, proportional to n_0, $n_0^{1/2}$, and n_0^0, respectively. The corresponding diagrams are shown in Fig. 1. A wavy line represents the Coulomb potential and each dotted line represents a factor $n_0^{1/2}$. The unperturbed ground state is then formally a vacuum. We now have a well-defined field-theory model.

B. The Propagators and the Dielectric Constant

The properties of the system of physical interest are summarized in a few propagators; e.g., the singularities of the Green's functions, the density, and the current propagators will give us the energies of some of the excited states. The long-range character of the Coulomb force is most effectively analyzed by introducing the dielectric constant. In the following we shall deduce, from the structure of the diagrams, the connections among the Green's functions, the density, and the current propagators and the dielectric constant.

An important notion in the dielectric constant approach is that of the "irreducible diagram." In this paper, we shall call a function *irreducible*, if every one of the diagrams contributing to it is an irreducible diagram, i.e., a diagram which is not made of two parts connected only by a single interaction line. In this paper, we shall use the word *proper* to denote the fact that a *proper diagram* is not made of two parts joined by a single one-particle line. For example, the self-energy diagrams are proper but may be reducible.

In the following analysis we shall define quite a few functions and derive many formulas (mainly through the summation of various geometric series). In order to clarify the motivation of such an analysis so that the physical meaning of these functions and formulas will be transparent, let us review briefly some of the well-known characteristics of a low-density system with a short-range interaction, and compare them to those for a charged Bose system.

A dilute system with a short-range interaction is conveniently characterized by two length parameters, the range of the force and the mean free path. The theory is usually concerned with the correlations or the propagations of various fluctuations over a distance comparable to or smaller than the mean free path (for those over a distance much larger than the mean free path, the macroscopic theory will take over). These propagations of fluctuations are mainly due to the motion of the particles; i.e., the energy and momentum generated by the source of fluctuations are carried by one or more particles to other parts of the system and give rise to the correlations. The interaction does not play a part directly in the correlations of fluctuations unless the distance involved is within the force range. Thus, the Green's function, which describes the propagation of a particle through the medium, plays the essential role in the theory. An analysis of the structure of the Green's function will reveal much physical characteristics of the system. The first step in analyzing the structure of the Green's function G is to express it in terms of the self-energy M by summing the geometric series

$$G=G_0+G_0MG_0+G_0MG_0MG_0+\cdots$$
$$=(G_0^{-1}-M)^{-1}, \quad (2.9)$$

where G_0 is the unperturbed Green's function. From a physical viewpoint, a great deal has been gained by

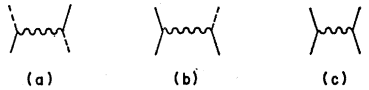

FIG. 1. The three types of interactions.

summing the geometric series, because, with formula (2.9), one does not have to know much about M to have a fairly clear picture of the single-particle propagation. For example, if the imaginary part of M is small, a Lorentzian-shape spectrum follows and a rough estimate of many quantities of physical interest such as the mean free path can be made. From a mathematical viewpoint, the summing of the whole geometric series is essential because any truncated series expansion of G is meaningless in the region near the singularities of G, which is often the region of interest. While G becomes singular, M is often well behaved. Then a truncated expansion for G^{-1} will be useful and the singularities of G may be studied approximately. In short, the summation of the geometric series (2.9) often allows one to construct a well-behaved perturbation expansion as well as to gain much physical insight to the problem. It is usually the only useful exact relation one can derive by a straightforward summation. The next step of the theory would be the analysis of the self-energy M and the other propagators constructed from G.

In contrast to a dilute system with a short-range interaction, the mean free path is no longer a useful concept for a charged system. The motion of a particle is constantly affected by all other particles through the instantaneous infinite-range Coulomb force. The propagations of fluctuations over any distance are mainly due to the long-range interaction instead of the motion of the particles. Roughly speaking, the particles now play the part which the interaction plays in the short-range case discussed above. They disturb the lines of force so that the "shielding length" plays the part of the mean free path in the short-range case. We want to emphasize that, unlike the mean free path in the dilute system discussed above, the concept of the shielding length in a charged system is not a concrete one. The modified Coulomb-interaction line still has an infinite range (i.e., proportional to $1/k^2$ for a small momentum transfer k) except at zero-energy transfer. In other words, only the *static* Coulomb field is shielded. The interaction with the modification of the medium is defined as the bare Coulomb potential *divided by* the dielectric constant. Thus, the dielectric constant is the fundamental concept in the theory. The density fluctuation is the source of the fluctuation of the Coulomb force. Thus the density propagator is closely related to the dielectric constant. For a Bose system, by (2.7), the density fluctuation is directly related to the single-particle amplitude as well as the two-particle amplitude. Therefore, the Green's function is also closely related to the dielectric constant. It is now clear that the dielectric constant plays the essential role in the theory of the charged Bose system. As the step equivalent to the summation of the geometric series for the Green's function in (2.9), we have to sum many geometric series involving the dielectric constant and the closely related propagators. Various proper irreducible functions will play the part of M in (2.9). Like (2.9), the results of summing these geometric series will enable us to gain much physical insight and to construct perturbation expansions which are well behaved near the singularities of the modified interaction line and of various propagators. Like the singularity of G_0 in (2.9), the $1/k^2$ singularity of the bare interaction line can cause no trouble after the geometric series are summed. We comment here that, because of the weakness (i.e., having no hard core) and the simple form of the Coulomb force, these geometric sums, which we now proceed to study, will display much more physical features for a charged Bose system than (2.9) does for a dilute system with a short-range interaction.

We now list our definitions of the propagators. We shall use script letters to denote the propagators. Irreducible functions will be denoted by capital letters. Unless otherwise specified, the arguments of the functions are always $(\mathbf{k}, \omega)$. For simplicity, we introduce the Greek indices, each assuming two values, $+$ and $-$, so that

$$\begin{aligned} a_k{}^{\mu} &= a_k, \qquad \text{if } \mu = +, \\ &= a_{-k}{}^{\dagger}, \qquad \text{if } \mu = -. \end{aligned} \tag{2.10}$$

The Green's functions form a 2×2 matrix.

$$\mathcal{G}_{\nu}{}^{\mu} = -i \int dt\, e^{i\omega t} \langle T(a_{\mathbf{k}}{}^{\mu}(t)\, a_{\mathbf{k}}{}^{\nu\dagger}) \rangle. \tag{2.11}$$

The density and current to single-particle amplitude propagators are defined as

$$\begin{aligned} \mathcal{C}_{\mu} &= -i \int dt\, e^{i\omega t} \langle T(\rho_{\mathbf{k}}(t)\, a_{\mathbf{k}}{}^{\mu\dagger}) \rangle, \\ \mathcal{C}^{\mu} &= -i \int dt\, e^{i\omega t} \langle T(a_{\mathbf{k}}{}^{\mu}(t)\, \rho_{\mathbf{k}}{}^{\dagger}) \rangle, \\ \mathcal{C}_{\mu}{}^{i} &= -i \int dt\, e^{i\omega t} \langle T(J_{\mathbf{k}}{}^{i}(t)\, a_{\mathbf{k}}{}^{\mu\dagger}) \rangle, \\ \mathcal{C}_{i}{}^{\mu} &= -i \int dt\, e^{i\omega t} \langle T(a_{\mathbf{k}}{}^{\mu}(t)\, J_{\mathbf{k}}{}^{i\dagger}) \rangle. \end{aligned} \tag{2.12}$$

The density and current propagators are

$$\begin{aligned} \mathcal{F}(\mathbf{k}, \omega) &= -i \int dt\, e^{i\omega t} \langle T(\rho_{\mathbf{k}}(t)\, \rho_{\mathbf{k}}{}^{\dagger}) \rangle, \\ \mathcal{F}^{i}(\mathbf{k}, \omega) &= -i \int dt\, e^{i\omega t} \langle T(J_{\mathbf{k}}{}^{i}(t)\, \rho_{\mathbf{k}}{}^{\dagger}) \rangle, \\ \mathcal{F}^{ij}(\mathbf{k}, \omega) &= -i \int dt\, e^{i\omega t} \langle T(J_{\mathbf{k}}{}^{i}(t)\, J_{\mathbf{k}}{}^{j\dagger}) \rangle. \end{aligned} \tag{2.13}$$

The indices i, j will always label the components of

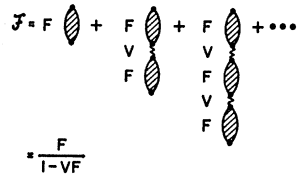

FIG. 2. The density propagator. A heavy dot represents a density vertex.

3 vectors. The function

$$-i\int dt\, e^{i\omega t}\langle T(\rho_k(t)J_k{}^{i\dagger})\rangle$$

can be shown[6] to be the same as $\mathfrak{F}^i$.

The following symmetry properties are easily deduced from the space and the time-inversion invariance of the system[6]:

$$\begin{aligned}
&\mathcal{G}_\nu{}^\mu=\mathcal{G}_\mu{}^\nu=\mathcal{G}_{-\mu}{}^{-\nu}(-\mathbf{k},-\omega),\\
&\mathcal{C}_\mu=\mathcal{C}^\mu=\mathcal{C}_{-\mu}(-\mathbf{k},-\omega),\\
&\mathcal{C}_\mu{}^i=\mathcal{C}_i{}^\mu=\mathcal{C}_{-\mu}{}^i(-\mathbf{k},-\omega),\\
&\mathfrak{F}=\mathfrak{F}(-\mathbf{k},-\omega)=\mathfrak{F}(-\mathbf{k},\omega),\\
&\mathfrak{F}^i=\mathfrak{F}^i(-\mathbf{k},-\omega)=-\mathfrak{F}^i(-\mathbf{k},\omega),\\
&\mathfrak{F}^{ij}=\mathfrak{F}^{ij}(-\mathbf{k},-\omega)=\mathfrak{F}^{ij}(-\mathbf{k},\omega)=\mathfrak{F}^{ji}.
\end{aligned}\tag{2.14}$$

Henceforth, all the propagators and the related irreducible functions are regarded as functions of complex ω. For real ω we let ω approach from above the real axis if $\omega>0$, and from below, if $\omega<0$.

The irreducible functions corresponding to the above propagators are $G_\nu{}^\mu$, C^μ, C_μ, $C_i{}^\mu$, $C_\mu{}^i$, F, F^i, and F^{ij}. They correspondingly satisfy the symmetry relations (2.14).

We now define the dielectric constant ϵ (not to be confused with the unperturbed single-particle energy $\epsilon_k=k^2/2m$) by

$$\mathfrak{F}=F/\epsilon.\tag{2.15}$$

Since $\mathfrak{F}$ is obtained from F by summing a geometric series (see Fig. 2), we see that

$$\epsilon=1-VF,\tag{2.16}$$

where $V=V_k=4\pi e^2/k^2$. It is easily seen from Fig. 2 that V/ϵ is the modified interaction line and (2.15) is equivalent to the previous definition of ϵ. It follows that

$$\begin{aligned}
&\mathfrak{F}^i=F^i/\epsilon,\\
&\mathfrak{F}^{ij}=F^{ij}+F^iF^jV/\epsilon.
\end{aligned}\tag{2.17}$$

The vertex functions Λ_ν, Λ^ν, $\Lambda_\nu{}^i$, $\Lambda_i{}^\nu$ are defined as (see Fig. 3)

$$\begin{aligned}
&C_\mu=\Lambda_\nu G_\mu{}^\nu,\\
&C_\mu{}^i=\Lambda_\nu{}^i G_\mu{}^\nu,\\
&C^\mu=G_\nu{}^\mu\Lambda^\nu,\\
&C_i{}^\mu=G_\nu{}^\mu\Lambda_i{}^\nu.
\end{aligned}\tag{2.18}$$

Repeated Greek indices are summed. The Λ's satisfy the symmetry relations for the C's in (2.14).

[6] The symmetry properties of the propagators are discussed in Ref. 5.

We further separate out the proper part of the F's (see Fig. 4) and write

$$\begin{aligned}
&F=\Lambda_\mu G_\nu{}^\mu\Lambda^\nu+F^r,\\
&F^i=\Lambda_\mu{}^i G_\nu{}^\mu\Lambda^\nu+F^{ir},\\
&F^{ij}=\Lambda_\mu{}^i G_\nu{}^\mu\Lambda_j{}^\nu+F^{ijr}.
\end{aligned}\tag{2.19}$$

The F^r's are proper as well as irreducible.

The cylindrical symmetry about the momentum $\mathbf{k}$ enables us to draw the following conclusions. Let the indices 1, 2 denote the transverse components of a 3 vector and 3 denote the longitudinal component. Then we have

$$\begin{aligned}
&\mathcal{C}_\mu{}^{1,2}=C_\mu{}^{1,2}=\Lambda_\mu{}^{1,2}=F^{1,2}=F^{1,2r}=0,\\
&\mathfrak{F}^{13}=\mathfrak{F}^{23}=F^{13}=F^{23}=F^{13r}=F^{23r}=0,\\
&\mathfrak{F}^{12}=F^{12}=F^{12r}=0.
\end{aligned}\tag{2.20}$$

It follows from (2.17), (2.19), (2.20) that

$$\mathfrak{F}^{11}=\mathfrak{F}^{22}=F^{11}=F^{22}=F^{11r}=F^{22r}.\tag{2.21}$$

Thus the full transverse-current propagators are proper and irreducible.

Let us now go back to the Green's functions. The self-energy $\mathfrak{M}$ (a 2×2 matrix) is defined through Dyson's equation:

$$\mathcal{G}^{-1}=G_0{}^{-1}-\mathfrak{M},\tag{2.22}$$

where G_0 is the unperturbed Green's function matrix:

$$\begin{aligned}
&G_{0+}{}^+=(\omega-\epsilon_k+\mu)^{-1},\\
&G_{0-}{}^+=0.
\end{aligned}\tag{2.23}$$

Let the numerator $\mathfrak{N}$ and the denominator $\mathfrak{D}$ be defined as

$$\begin{aligned}
&\mathfrak{D}=-\det|\,\mathcal{G}^{-1}\,|,\\
&\mathcal{G}=\mathfrak{N}/\mathfrak{D}.
\end{aligned}\tag{2.24}$$

Clearly, $\mathfrak{M}$ and $\mathfrak{N}$ have the same symmetry properties that $\mathcal{G}$ has, [see (2.14)]. Let

$$\begin{aligned}
&\mathcal{S}\equiv\tfrac{1}{2}(\mathfrak{M}_+{}^+ +\mathfrak{M}_-{}^-),\ \mathcal{A}\equiv\tfrac{1}{2}(\mathfrak{M}_+{}^+ -\mathfrak{M}_-{}^-),\\
&\mathfrak{M}_2\equiv\mathfrak{M}_-{}^+.
\end{aligned}\tag{2.25}$$

Then

$$\begin{aligned}
&\mathfrak{N}_+{}^+=\omega+\epsilon_k-\mu+\mathfrak{M}_-{}^-,\\
&\mathfrak{N}_-{}^+=-\mathfrak{M}_2,\\
&\mathfrak{D}=(\omega-\mathcal{A})^2-(\epsilon_k-\mu+\mathcal{S}-\mathfrak{M}_2)(\epsilon_k-\mu+\mathcal{S}+\mathfrak{M}_2).
\end{aligned}\tag{2.26}$$

We define N, D, M, S, A, M_2 as the irreducible functions

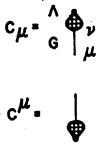

FIG. 3. The irreducible density (or current) to single-particle amplitude propagator. The heavy dots are density (or current) vertices.

corresponding to $\mathfrak{N}$, $\mathfrak{D}$, $\mathfrak{M}$, $\mathfrak{S}$, $\mathfrak{A}$, $\mathfrak{M}_2$. Equations (2.22), (2.24), (2.25), and (2.26) remain valid with the script letters replaced by the corresponding capital letters. The functions N, D, M, S, A, M_2 are all both proper and irreducible.

Now it is a straightforward matter to combine irreducible functions to obtain the functions represented by script letters. By Fig. 5, the self-energy $\mathfrak{M}$ may be written as

$$\mathfrak{M}_\nu{}^\mu = \Lambda^\mu \Lambda_\nu V/\epsilon^r + M_\nu{}^\mu,$$
$$\epsilon^r \equiv 1 - VF^r. \tag{2.27}$$

We may not use the full dielectric constant ϵ here because the single isolated one-particle lines are excluded from $\mathfrak{M}$.

Substituting (2.27) in (2.26), we obtain

$$\mathfrak{D} = D - (V/\epsilon^r)\Lambda_\mu N_\nu{}^\mu \Lambda^\nu. \tag{2.28}$$

Since the dielectric constant is, by (2.16), (2.19),

$$\epsilon = 1 - VF$$
$$= 1 - V(\Lambda_\mu G_\nu{}^\mu \Lambda^\nu + F^r), \tag{2.29}$$

Eq. (2.28) becomes

$$\mathfrak{D} = (\epsilon/\epsilon^r) D. \tag{2.30}$$

We now summarize our results by expressing the propagators in terms of the dielectric constant and the irreducible functions.

$$\mathfrak{G}_\nu{}^\mu = \epsilon^{-1}(\epsilon^r G_\nu{}^\mu + (V/D)\mu\nu\Lambda^{-\mu}\Lambda_{-\nu}), \tag{2.31}$$
$$\mathfrak{C}_\mu = \Lambda_\nu G_\mu{}^\nu/\epsilon,$$
$$\mathfrak{C}_\mu{}^3 = (F^3(V/\epsilon)\Lambda_\nu + \Lambda_\nu{}^3) G_\mu{}^\nu, \tag{2.32}$$
$$\mathfrak{F} = F/\epsilon,$$
$$\mathfrak{F}^3 = F^3/\epsilon,$$
$$\mathfrak{F}^{33} = F^{33} + F^3 F^3 V/\epsilon. \tag{2.33}$$

(2.31) is obtained through Eqs. (2.24)–(2.29). The Eqs. (2.32) are easily seen from Fig. 6. Equations (2.33) are just (2.15), (2.17). The above propagators involve the single-particle amplitude and the longitudinal current. Both are invariant under the rotation about $\mathbf{k}$. The nonvanishing transverse-current propagators are, by (2.21),

$$\mathfrak{F}^{11} = \mathfrak{F}^{22} = F^{11r} = F^{22r}. \tag{2.34}$$

While (2.34) is a trivial identify for any system (with no tensor force) and (2.33) holds for any charged system, Fermi or Bose, the results (2.31) and (2.32)

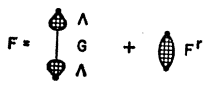

FIG. 4. The irreducible density (or current) propagator. The heavy dots are density (or current) vertices.

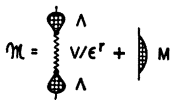

FIG. 5. The self-energy in terms of irreducible functions.

are unique for a charged Bose system. For a charged Fermi system, the density or current does not couple to the single-particle operators, i.e., $\Lambda_\mu = \Lambda_\mu{}^i = 0$. Thus, speaking loosely, for a Fermi system, one would have

$$F = F^r, \qquad \epsilon = \epsilon^r, \qquad \mathfrak{G} = G, \qquad \mathfrak{C} = 0, \tag{2.35}$$

so that the Green's functions would be irreducible and would not depend on the dielectric constant explicitly. In the Bose system, as is shown by (2.31), the dielectric constant plays an essential role in the structure of the Green's functions, although it does not, according to (2.34), affect the transverse propagators directly. We shall discuss these points more fully in the next section.

C. Some Consequences of the Continuity Equation

The propagators involving the longitudinal current $J_{\mathbf{k}}{}^3$ are related to those involving the density fluctuation $\rho_{\mathbf{k}}$ through the continuity equation

$$i\,(\partial\rho_{\mathbf{k}}/\partial t) = kJ_{\mathbf{k}}{}^3. \tag{2.36}$$

By taking the time derivatives of the propagators and keeping track of the discontinuity due to the time ordering, one easily obtains from (2.13)

$$\omega\mathfrak{F} = k\mathfrak{F}^3,$$
$$\omega\mathfrak{F}^3 = k[\mathfrak{F}^{33} + (n/m)]. \tag{2.37}$$

By (2.15), (2.17), we see that

$$\omega F = kF^3,$$
$$\omega F^3 = k[F^{33} + (n/m)]. \tag{2.38}$$

Thus

$$\mathfrak{F} = (k^2/\omega^2)[\mathfrak{F}^{33} + (n/m)],$$
$$F = (k^2/\omega^2)[F^{33} + (n/m)]. \tag{2.39}$$

From (2.12), we obtain

$$\omega\mathfrak{C}_\mu = k\mathfrak{C}_\mu{}^3 + (\sqrt{n_0})\beta_\mu, \tag{2.40}$$

where

$$\beta_\mu = 1 \qquad \text{for } \mu = +,$$
$$= -1 \qquad \text{for } \mu = -. \tag{2.41}$$

The term $(n_0)^{1/2}\beta_\mu$, comes from the commutator

$$[\rho_{\mathbf{k}}, a_{\mathbf{k}}{}^{\mu\dagger}] = (n_0)^{1/2}\beta_\mu. \tag{2.42}$$

Using (2.32) and (2.40), we obtain

$$\omega\Lambda_\nu G_\mu{}^\nu = k\Lambda_\nu{}^3 G_\mu{}^\nu + (n_0)^{1/2}\beta_\mu. \tag{2.43}$$

Similarly,

$$\omega G_\nu{}^\mu \Lambda^\nu = kG_\nu{}^\mu \Lambda_3{}^\nu + (n_0)^{1/2}\beta^\mu, \tag{2.44}$$

where $\beta^\mu = \beta_\mu$. (2.43) and (2.44) are the same since

$$\Lambda_\mu = \Lambda^\mu, \qquad G_\mu{}^\nu = G_\nu{}^\mu.$$

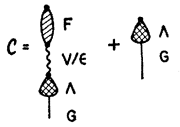

FIG. 6. The full density (or current) to single-particle amplitude propagator in terms of irreducible functions.

From the definition of F^r, F^{ir}, F^{ijr} [see (2.19)] and the Eqs. (2.38, 2.43, 2.44), we can express the relationship among F^r, F^{3r} and F^{33r} as

$$\omega F^r = kF^{3r} - (n_0)^{1/2}\beta_\nu \Lambda^\nu, \tag{2.45}$$

$$\omega F^{3r} = k(F^{33r} + (n/m)) - (n_0)^{1/2}\Lambda_\mu{}^3\beta^\mu, \tag{2.46}$$

thus

$$F^r = (k^2/\omega^2)(F^{33r} + (n/m)) - [(n_0)^{1/2}/\omega^2](k\Lambda_\mu{}^3 + \omega\Lambda_\mu)\beta^\mu. \tag{2.47}$$

The formulas (2.37)–(2.39) apply also to a Fermi system while (2.43)–(2.47) are meaningful only for a Bose system. These formulas derived above from the continuity equation may be referred to as the Ward identities.

So far we have been able to express the dielectric constant and the full propagators in terms of the functions Λ, M, N and etc., which are proper and irreducible. In other words, we have analyzed the role of the isolated single-interaction line and that of the isolated single-particle line by summing a few geometric series. The next step is then the study of the isolated pair of lines and, instead of the geometric series, one would encounter the Bethe–Salpeter-type equations. The kernels of the integral equations and the vertex functions will play the role of the irreducible functions in the geometric sums. We shall make no attempt to analyze the structure of the Bethe–Salpeter equations in this paper.

III. QUALITATIVE FEATURES OF THE EXCITED STATES

The qualitative features of the excited states are easily understood in terms of the perturbation theory. As in the case of an electron gas, there is only one dimensionless parameter in the theory, i.e., r_s, the ratio of the average interparticle distance to the Bohr radius. By choosing the appropriate system of units, as will be seen in the next section, the parameter of the perturbation expansion becomes proportional to $r_s^{3/4}$. Therefore, if the density is high enough so that the perturbation expansion converges, we expect the physical picture to be that given by the lowest-order approximation, i.e., the Bogoliubov approximation, with some modifications which may be regarded as small. We can then apply the exact formal results derived in the previous section to obtain a consistent description of the excited states. The physical meaning of these formal results then becomes more transparent. In this section, a general description will be followed by a brief discussion of the analytic behavior of the various functions defined in the previous section and of some characteristic features of the excited states at small momenta.

A. General Description

In a Fermi gas, transitions between a state with an even number of particles and a state with an odd number of particles are forbidden. The situation is quite different for a Bose gas. The presence of the condensate, which is a classical field in our model, in the Bose system implies that the transition between a one-particle state and a two-particle state is allowed, and hence that the transition between two states with any number of particles is allowed unless it is forbidden by symmetry.

Therefore, the singularities of the Green's functions $\mathcal{G}_\nu{}^\mu(\mathbf{k}, \omega)$ give the energies of *all* those excited states with momentum $\mathbf{k}$ and zero angular momentum along the vector $\mathbf{k}$, i.e., zero helicity. The density propagator and the longitudinal current propagator share the same singularities with $\mathcal{G}$, since they all have the same symmetry. This fact is already demonstrated to some extent by our previous results (2.31)–(2.33). The transverse-current propagator is singular at the energies of those excited states with helicity ± 1. Similarly, one can construct tensor operators with helicities ± 2, ± 3, ± 4, and so on. The singularities of the corresponding propagators will then give the excited-state energies of the corresponding helicities.

In the Bogoliubov approximation (which will be discussed more quantitatively later), a single quasiparticle with momentum $\mathbf{k}$ has the energy

$$(\epsilon_k{}^2 + \omega_{\rm pl}{}^2)^{1/2} \equiv E_k{}^B, \tag{3.1}$$

where $\omega_{\rm pl} = (4\pi ne^2/m)^{1/2}$ is the plasma frequency. ϵ_k is the unperturbed single-particle energy $k^2/2m$ [see (2.2)], not to be confused with the dielectric constant ϵ. The quasiparticle has zero helicity. The finite energy gap $\omega_{\rm pl}$ is easily understood. The interference between the particle amplitude and the amplitude of the zero-momentum oscillator, the condensate, always produces a density fluctuation, which implies a charge separation. The electrostatic restoring force then comes in to play and raises the energy.

Any excited state, in this approximation, is made of

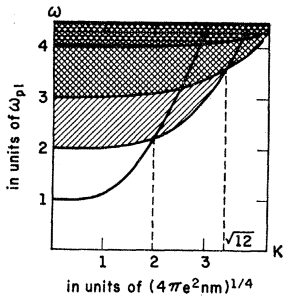

FIG. 7. The energy levels in the Bogoliubov approximation. The cutoff momentum is at $k=2$.

one or more of these noninteracting quasiparticles. The energy levels versus the momentum is shown in Fig. 7. We see that the lowest excited state is a single quasiparticle state if k is less than 2, measured in units of $(4\pi nme^2)^{1/4}$. The two-particle continuum starts at the threshold $2E_{k/2}{}^B$, which corresponds to two quasiparticles each having momentum $\mathbf{k}/2$. The three-particle continuum starts at the three particle threshold $3E_{k/3}{}^B$, and so on. For k larger than 2, which is the *cutoff momentum*, beyond which no discrete level exists, the two-particle threshold becomes lower than the single-particle energy $E_k{}^B$. For k larger than $(12)^{1/2}$, the three-particle threshold becomes lower than the two-particle threshold, and so on.

It is straightforward to construct a state of any helicity and momentum from the states of two or more quasiparticles by superposition. The important feature is that the states with helicity greater or equal to 1 must be a state with at least two quasiparticles and therefore have an energy greater than two times the plasma frequency. There are no low-lying transverse excitations. One might argue that there should be flow patterns which involve no charge separation (i.e., purely shear flow), and thus have lower energy than the plasma frequency. However, such a flow pattern would mean that the condensate flows also. This type of motion, which is hydrodynamic in nature, is not included in the present theory, which assumes a macroscopic occupation of the zero-momentum state, i.e., a stationary condensate. We shall not study the case of a moving condensate here.

To go beyond the Bogoliubov approximation, we turn on the interaction between the quasiparticles. The above-described features will be modified. The single quasiparticle energy will be shifted and hence the 2-particle, 3-particle, etc., thresholds will be shifted. The cutoff momentum will be shifted. For k larger than the cutoff momentum, the single quasiparticle becomes unstable and will decay into 2 or more quasiparticles with momenta less than the cutoff momentum. Besides the decay processes, there will be scattering processes. The important question is whether the bound states of two or more quasiparticles can occur. If they do occur, the above description would have to be modified to a great extent. One can easily verify that the interaction between two quasiparticles is repulsive. Therefore, the bound states are likely to be absent.

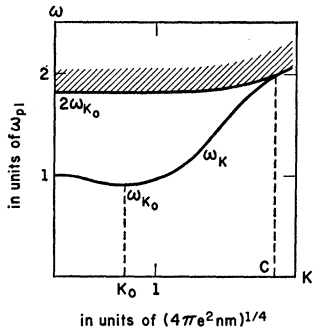

FIG. 8. A rough sketch of the low-lying energy levels for $r_s\sim 2$. The lowest-excited-state energy occurs at $k=k_0$. C is the cutoff momentum.

Thus, the modified-excitation spectrum consists of a single dispersion curve ω_k, the shifted quasiparticle energy, below the cutoff momentum plus a continuum. The boundary of the continuum, i.e., the threshold energy as a function of k, will be denoted by $E_{\rm thr}(k)$. It will be shown later that the dispersion curve ω_k will have a minimum ω_{k_0} at a finite momentum k_0(see Fig. 8). Thus, for k less than $2k_0$,

$$E_{\rm thr}(k)=2\omega_{k_0}. \tag{3.2}$$

For k greater than $2k_0$, $E_{\rm thr}(k)$ has to be obtained from $2\omega_{k/2}$, or $3\omega_{k/3}$, $\cdots$ whichever is the smallest.

B. Analytic Behavior

In view of the above discussion, the analytic behavior of all the functions we have studied in the previous section can be easily deduced.

Since the singularities of all the propagators are located symmetrically about the origin, it is more convenient to use the ω^2 plane instead of the ω plane.

Below the cutoff momentum, for all the zero-helicity propagators, there is a pole at $\omega_k{}^2$ and a cut starting from the threshold $E_{\rm thr}{}^2(k)$ to infinity, i.e., a branch point at $E_{\rm thr}{}^2(k)$. Above the cutoff momentum, there is no simple pole, but a branch point at $E_{\rm thr}{}^2(k)$ for all the propagators. In both cases, there are additional branch points above $E_{\rm thr}{}^2(k)$ at the thresholds of multiparticle states. We shall not be interested in them.

The transverse current propagator $\mathfrak{F}^{11}=\mathfrak{F}^{22}=\mathfrak{F}^{r11}$ and the functions M, N, Λ, Λ^i, F^r, F^{ir}, and F^{ijr} are constructed from diagrams involving at least two quasiparticles. Since there is no bound state, these functions have no simple pole. They all share the cut starting from $E_{\rm thr}{}^2(k)$.

It is now clear that, by Eqs. (2.31), (2.32), (2.33), (2.39), and (2.40), the simple pole of the zero-helicity propagators $\mathcal{G}$, $\mathcal{C}$, $\mathcal{C}^3$, $\mathfrak{F}$, $\mathfrak{F}^3$, and $\mathfrak{F}^{33}$ must be the zero of the dielectric constant. The poles of G (i.e., the zeroes of D), do not give rise to any pole of the full propagators because they are also the poles of the dielectric constant [see (2.29)].

The branch point $\omega^2=E_{\rm thr}{}^2(k)$ is common to all the functions we have studied although the nature of the branch point may differ from one function to another. We shall not study the precise threshold behavior of the functions but only give the following estimate in terms of the density of the two-particle states for a two-particle threshold. A similar estimate may be made for a many-particle threshold in terms of the density of many-particle states. Consider a proper irreducible function, e.g., F^r. Near the branch point the disconti-

nuity across the cut is

$$F^r(\omega+i\eta)-F^r(\omega-i\eta)$$
$$=-i\int\frac{d^3p}{(2\pi)^3}\,2\pi\delta(\omega-\omega_{-p+k/2}-\omega_{p+k/2})$$
$$\times(\text{a slowly varying function of }\omega)$$
$$\sim\theta(\omega-E_{\text{thr}}(k))\rho_2(\omega), \tag{3.3}$$

where ρ_2 is the density of the two-particle states near the threshold. For k greater than $2k_0$,

$$\rho_2(\omega)\sim(m^*)^{3/2}(\omega-2\omega_{k/2})^{1/2}, \tag{3.4}$$

where

$$1/m^*=(d^2\omega_p/dp^2)_{p=k/2} \tag{3.5}$$

measures the curvature of the dispersion curve at $\frac{1}{2}k$. For k less than $2k_0$,

$$\rho_2=\text{a constant}. \tag{3.6}$$

Therefore, at the two-particle threshold, the branch point for a proper irreducible function is either a square-root singularity or a logarithmic singularity.

C. The Dispersion Curve at Very Small Momenta

We proceed to derive an inequality which must be satisfied by ω_k for small k. The irreducible functions are all related to the thermodynamic derivatives as ω and k approach zero. We emphasize that, for a charged system, the thermodynamic derivatives are related to the *irreducible functions*, not the general propagators. This is because the interaction line V_k for $k=0$ is excluded owing to the uniform neutralizing charge background so that any ground-state diagram is irreducible. It can be shown that, for small ω and k,

$$F=(nk^2/m)(\omega^2-c^2k^2)^{-1}. \tag{3.7}$$

The proof of (3.7) is given in Ref. 5.[7] The quantity c^2 is defined by

$$mc^2=n(d\mu/dn). \tag{3.8}$$

If c^2 is greater than zero, c may be interpreted as the speed of sound. In the present case, c^2 is less than zero, as will be seen in the next section.

Equation (3.7) is in fact valid for all ω because it has exhausted the f sum rule, which states that the total weight of the spectrum of $\mathfrak{F}$ (and hence that of F) is nk^2/m. Thus, for any ω, we have

$$F=(1-\delta)(nk^2/m)(\omega^2-c^2k^2)^{-1}+F', \tag{3.9}$$

where

$$\delta\to 0,$$
$$F'/k^2\to 0, \tag{3.10}$$

as k approaches zero. F' is the contribution from the continuum. The dielectric constant is then

$$\epsilon=1-(4\pi e^2/k^2)F$$
$$=(\omega^2-c^2k^2)^{-1}(\omega^2-c^2k^2-\omega_{p1}^2+\omega_{p1}^2\delta$$
$$-(4\pi e^2F'/k^2)(\omega^2-c^2k^2)). \tag{3.11}$$

Now, $\delta>0$, as required by the f sum rule and, for ω less than the threshold, $F'<0$. Therefore, we have the following inequality for ω_k, which is the zero of ϵ:

$$\omega_k^2-\omega_{p1}^2<c^2k^2. \tag{3.12}$$

This inequality will provide a check on any calculation of the dispersion curve near $k=0$. Furthermore, we see that in the limit of infinitesimal momentum, ω_k must be *precisely* the plasma frequency. This fact is well known for an electron gas. Since c^2 is less than zero, the negative curvature of the dispersion curve implies that a minimum exists for the dispersion curve at $k=k_0$. Thus, the two-particle states with the lowest energy will be those made of two particles each having a momentum of magnitude k_0. Therefore, the threshold is flat for $k<2k_0$, i.e.,

$$E_{\text{thr}}(k)=2\omega_{k_0}, \qquad \text{for } k<2k_0. \tag{3.13}$$

The energy $2\omega_{k_0}$ must be greater than the plasma frequency, because otherwise the small-momentum quasiparticles would be unstable and hence would not have a precisely defined frequency.

IV. CALCULATIONS

A. Units

In this section, we shall determine the dispersion curve below the cutoff momentum to the next order beyond the Bogoliubov approximation.

We shall use the system of units in which the momentum or the inverse length is measured in $(4\pi nme^2)^{1/4}$ and the energy is measured in the plasma frequency $\omega_{p1}=(4\pi ne^2/m)^{1/2}$. Let the coupling constant g be defined as

$$g=(4\pi)^{3/4}(e^6m^3/n)^{1/4}=4\pi r_s^{3/4}/3^{1/4}. \tag{4.1}$$

In the new system of units, we have

$$m=1,$$
$$4\pi e^2=n^{-1}=g. \tag{4.2}$$

Here g is the parameter of the perturbation expansion.

The orders of magnitude of the quantities concerning us are listed in the following: The number of particles excluding the condensate, $n'=O(1)$, the chemical potential $\mu=O(g)$, the dielectric constant $\epsilon=O(1)$, the irreducible Green's functions $G_+{}^+=O(1)$, $G_-{}^+=O(g)$, the irreducible self-energy $M=O(g)$, the irreducible density and current propagators $F=O(g^{-1})$, $F^r=O(1)$, and the vertex function $\Lambda=O(g^{-1/2})$.

[7] Although their analysis is for a neutral Bose system, it is completely applicable (and, in fact, more rigorously here because of the finite energy gap) to the irreducible functions.

The task is to solve the equation

$$\epsilon(\mathbf{k}, \omega_k) = 1 - (4\pi e^2/k^2) F(\mathbf{k}, \omega_k) = 0 \qquad (4.3)$$

for ω_k. It turns out that it is more convenient for computation to express F in terms of F^{33}. Substituting (2.39) in (4.3), we have, in the new system of units,

$$\epsilon(\mathbf{k}, \omega_k) = 1 - (1/\omega_k^2)\,(1 + gF^{33}(\mathbf{k}, \omega_k)) = 0. \qquad (4.4)$$

Equation (2.19) gives

$$F^{33} = \Lambda_\mu{}^3 G_\nu{}^\mu \Lambda_3{}^\nu + F^{33r}. \qquad (4.5)$$

The perturbation expansion of the dispersion curve has the form

$$\omega_k = \omega_k{}^{(0)} + g\omega_k{}^{(1)} + g^2\omega_k{}^{(2)} + \cdots. \qquad (4.6)$$

Substituting (4.6) in (4.4), expanding in powers of g, and setting the coefficients to zero, one then obtains the equations for $\omega_k{}^{(0)}$, $\omega_k{}^{(1)}$, and so on. However, the expansion is not meaningful unless ω_k is away from the singularities of $\epsilon(\mathbf{k}, \omega)$. As was shown in the previous section, every function involved in (4.5) has a branch point at $\omega^2 = E_{\text{thr}}{}^2(k)$. Thus, the expansion is not meaningful when ω_k is close to $E_{\text{thr}}(k)$, i.e., when k is close to the cutoff momentum. Above the cutoff momentum, $\epsilon(\mathbf{k}, \omega)$ has no zero. However, one can analytically continue ϵ across the cut and solve (4.3) for a complex ω_k, which may be interpreted as the energy of an unstable quasiparticle. Besides the branch point, ϵ also has a pole located at the pole of G. This singularity is always far away from ω_k and causes no difficulty.

B. The Bogoliubov Approximation

In this approximation, only the lowest-order quantities are kept. (See Fig. 9.) We have

$$\begin{aligned} &n_0 = n = g^{-1}, \\ &\Lambda_\mu = \sqrt{n_0} = g^{-1/2}, \\ &\Lambda_\mu{}^3 = \sqrt{n_0}(k/2m)\beta_\mu = g^{-1/2}\beta_\mu \tfrac{1}{2}k, \\ &G_+{}^+ = (\omega - \epsilon_k)^{-1}, \\ &G_-{}^+ = 0, \\ &\mu = 0, \qquad n' = 0, \\ &F^{33r} = 0, \end{aligned} \qquad (4.7)$$

where β_μ is defined by (2.41). Substituting (4.7) in

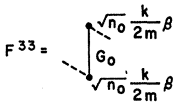

FIG. 9. The irreducible longitudinal current propagator in the lowest-order approximation.

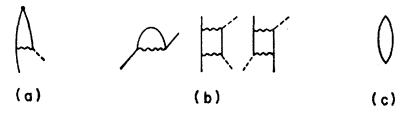

FIG. 10. The 1-ring diagrams. (a) The longitudinal-current vertex Λ^3. (b) The self-energy M. (c) The proper irreducible F^{33r}.

(4.5), one has

$$F^{33} = g^{-1}\tfrac{1}{4}k^2(G_+{}^+ + G_-{}^-) = g^{-1}\epsilon_k{}^2/(\omega^2 - \epsilon_k{}^2). \qquad (4.8)$$

Thus

$$\epsilon = 1 - (1/\omega^2)\,(1 + (\epsilon_k{}^2/\omega^2 - \epsilon_k{}^2)) = 1 - (\omega^2 - \epsilon_k{}^2)^{-1}.$$

The lowest-order ω_k is then given by $\epsilon(\mathbf{k}, \omega_k) = 0$, i.e.,

$$\omega_k{}^{(0)} = [1 + \epsilon_k{}^2]^{1/2} \equiv E_k{}^B. \qquad (4.9)$$

The full Green's functions in this approximation are, by (2.31),

$$\mathcal{G}_\nu{}^\mu = \epsilon^{-1}(G_\nu{}^\mu + (\mu\nu/Dk^2)). \qquad (4.10)$$

A little algebra shows that

$$\begin{aligned} &\mathcal{G}_+{}^+ = [(1+n_k)/(\omega - E_k{}^B)] - [n_k/(\omega + E_k{}^B)], \\ &\mathcal{G}_-{}^+ = -\bar{n}_k((\omega - E_k{}^B)^{-1} - (\omega + E_k{}^B)^{-1}), \end{aligned} \qquad (4.11)$$

where

$$\begin{aligned} &n_k = \langle a_{\mathbf{k}}{}^\dagger a_{\mathbf{k}}\rangle = (2E_k{}^B)^{-1}(\epsilon_k - E_k{}^B + (1/k^2)), \\ &\bar{n}_k = -\langle a_{\mathbf{k}} a_{-\mathbf{k}}\rangle = -\langle a_{\mathbf{k}}{}^\dagger a_{-\mathbf{k}}{}^\dagger\rangle = (2E_k{}^B k^2)^{-1}. \end{aligned} \qquad (4.12)$$

n_k and $\bar{n}_k$ are related to the original Bogoliubov transformation

$$a_{\mathbf{k}} = A_k \alpha_{\mathbf{k}} - B_k \alpha_{-\mathbf{k}}{}^\dagger$$

through

$$A_k{}^2 = 1 + n_k, \qquad B_k{}^2 = n_k, \qquad A_k B_k = \bar{n}_k. \qquad (4.13)$$

C. First-Order Approximations

In this approximation, we also keep those diagrams with one "ring," the first-order chemical potential, and the zeroth-order n'. The one-ring diagrams are shown in Fig. 10, (a) is for Λ^3, (b) for the self-energy M, and (c) for F^{33r}. The solid lines in the diagrams are the full zeroth-order Green's functions given by (4.11). The one-ring diagrams exhaust all the first-order contributions to ϵ.

Let $n_0{}^{1/2}(4\pi e^2)^{1/2}\Gamma_\mu$ be defined as the 1-ring contribution to $\Lambda_\mu{}^3$, then

$$\Lambda_\mu{}^3 = \sqrt{n_0}\tfrac{1}{2}k\beta_\mu + \Gamma_\mu(n_0)^{1/2}(4\pi e^2)^{1/2}. \qquad (4.14)$$

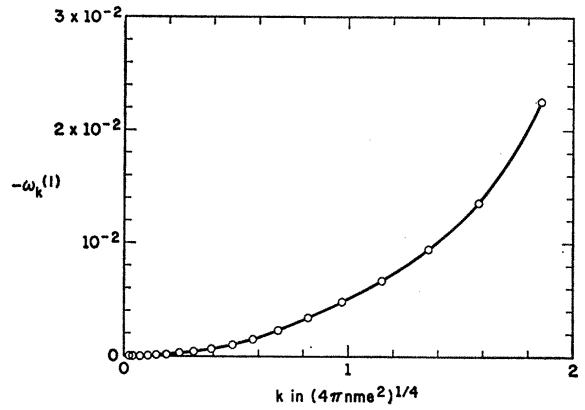

FIG. 11. The first-order energy shift. To this order, the dispersion curve is given by $\omega_k=(E_k{}^B+g\omega_k{}^{(1)})\omega_{\rm pl}$. The parameter g is related to r_s by $g=4\pi r_s{}^{3/4}/3^{1/4}$. Notice that $\omega_k{}^{(1)}$ is negative.

The factor $\sqrt{n_0}(4\pi e^2)^{1/2}$ takes care of the interaction line and the condensate line in Fig. 10(a). Recall that $4\pi e^2=n^{-1}=g$, and $n_0=n-n'$; thus

$$\Lambda_\mu{}^3\Lambda_3{}^\nu=g^{-1}\tfrac{1}{4}k^2\beta_\mu\beta^\nu-n'\tfrac{1}{4}k^2\beta_\mu\beta^\nu+\tfrac{1}{2}k(\beta_\mu\Gamma^\nu+\Gamma_\mu\beta^\nu). \tag{4.15}$$

The irreducible Green's functions are given by, to the first order,

$$\begin{aligned}G(k,\omega_k)&=N/D\\&=(N^{(0)}+gN^{(1)})/(D^{(0)}+gD^{(1)})\\&=G^{(0)}(\mathbf{k},\omega_k)+(g/D^{(0)})\,(N^{(1)}-(D^{(1)}/D^{(0)})N^{(0)}).\end{aligned} \tag{4.16}$$

Substituting (4.15), (4.16) in (4.5) and (4.4), and noticing that

$$D^{(0)}(k,E_k{}^B)=E_k{}^{B2}-\epsilon_k{}^2=1,$$

we obtain

$$\begin{aligned}\omega_k{}^2-E_k{}^{B2}=(g/E_k{}^{B2})[&-n'\epsilon_k{}^2+\tfrac{1}{4}k^2\beta_\mu N_\nu{}^{(1)\mu}\beta^\nu\\&+\tfrac{1}{2}k(\beta_\mu N_\nu{}^{(0)\mu}\Gamma^\nu+\Gamma_\mu N_\nu{}^{(0)\mu}\beta^\nu)\\&-D^{(1)}\tfrac{1}{4}k^2\beta_\mu N_\nu{}^{(0)\mu}\beta^\nu+F^{33r}].\end{aligned} \tag{4.17}$$

The explicit expressions for N, D are given by (2.26) with the script letters replaced by the corresponding capital letters. Keeping terms to the first order, we find

$$\begin{aligned}N_+{}^{(1)+}&=-\mu^{(1)}+M_-{}^{(1)-},\\N_-{}^{(1)+}&=-M_2{}^{(1)},\\D^{(1)}&=-2\omega A^{(1)}-2\epsilon_k(S^{(1)}-\mu^{(1)}).\end{aligned} \tag{4.18}$$

Substituting (4.18) in (4.17), we have

$$\begin{aligned}\omega_k{}^2-E_k{}^{B2}=(g/E_k{}^{B2})\{&-n'\epsilon_k{}^2+\epsilon_k(S^{(1)}+M_2{}^{(1)}-\mu^{(1)})\\&+k[E_k{}^B(\Gamma_++\Gamma_-)+\epsilon_k(\Gamma_+-\Gamma_-)]\\&+2\epsilon_k{}^2[E_k{}^BA^{(1)}+\epsilon_k(S^{(1)}-\mu^{(1)})]+F^{33r}\}\\\equiv 2E_k{}^Bg\omega_k{}^{(1)}.\end{aligned} \tag{4.19}$$

It is a straightforward matter to write down the contributions of the diagrams shown in Fig. 10. We find, after some algebra,

$$S^{(1)}=\frac{1}{4}\int\frac{d^3p}{(2\pi)^3}V_{\rm p+k}(\lambda_{\rm p}-1)^2/\lambda_{\rm p}+\frac{1}{4}\int\frac{d^3p}{(2\pi)^3}V_p[V_p\lambda_p/\lambda_{\rm p+k}+V_{\rm p+k}+\lambda_{\rm p}\lambda_{\rm p+k}(V_{\rm p}+V_{\rm p+k})]Q^+,$$

$$S^{(1)}+M_2{}^{(1)}=\frac{1}{2}\int\frac{d^3p}{(2\pi)^3}V_{\rm p}(\lambda_{\rm p+k}-1)+\frac{1}{2}\int\frac{d^3p}{(2\pi)^3}V_{\rm p}\lambda_{\rm p+k}\lambda_{\rm p}(V_{\rm p}+V_{\rm p+k})Q^+,$$

$$A^{(1)}=\frac{1}{2}\int\frac{d^3p}{(2\pi)^3}V_{\rm p}\lambda_{\rm p}(V_{\rm p}+V_{\rm p+k})Q^-,$$

$$\Gamma_++\Gamma_-=\frac{1}{2}\int\frac{d^3p}{(2\pi)^3}V_{\rm p}(\lambda_{\rm p}-\lambda_{\rm p+k})\,(\mathbf{p}\cdot\hat{k}+\tfrac{1}{2}k)Q^-,$$

$$\Gamma_+-\Gamma_-=\frac{1}{2}\int\frac{d^3p}{(2\pi)^3}V_{\rm p}(\lambda_{\rm p}/\lambda_{\rm p+k}-1)\,(\mathbf{p}\cdot\hat{k}+\tfrac{1}{2}k)Q^+,$$

$$F^{33r}=\frac{1}{4}\int\frac{d^3p}{(2\pi)^3}\lambda_{\rm p}{}^{-1}(1-\lambda_{\rm p})\,(\lambda_{\rm p+k}-\lambda_{\rm p})\,(\mathbf{p}\cdot\hat{k}+\tfrac{1}{2}k)^2Q^+, \tag{4.20}$$

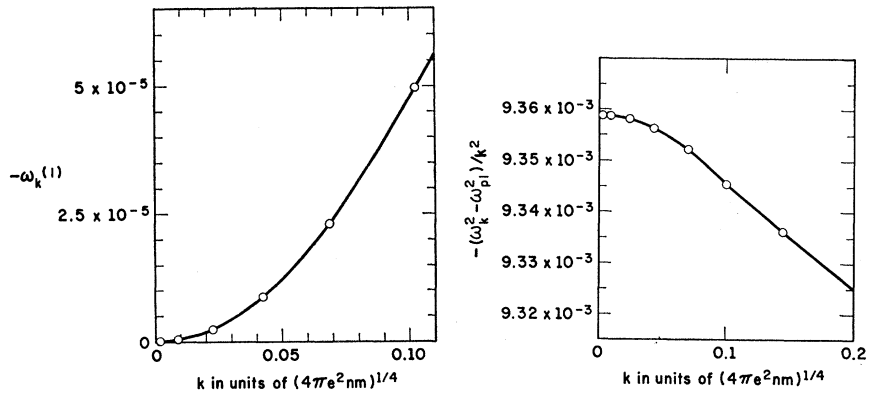

FIG. 12. The energy shift at small momenta. (a) $-\omega_k^{(1)}$ versus k. (b) $-(\omega_k^2-\omega_{pl}^2)/k^2$ in units of $g(4\pi ne^2/m^3)^{1/2}$.

where

$$Q^{\pm}\equiv(E_k^B-E_{p+k}^B-E_p^B)^{-1}\mp(E_k^B+E_{p+k}^B+E_p^B)^{-1},$$

$$\lambda_p\equiv\epsilon_p/E_p^B=\tfrac{1}{2}p^2(\tfrac{1}{4}p^4+1)^{-1/2}, \tag{4.21}$$

and $V_p=1/p^2$. The n' is given by

$$n'=\int\frac{d^3p}{(2\pi)^3}n_p=2.2139\times10^{-2}, \tag{4.22}$$

and the chemical potential $\mu=g\mu^{(1)}$ can be obtained by differentiating the lowest-order ground-state energy with respect to n, or from the Hugenholtz–Pines theorem[4]:

$$\mu^{(1)}=S^{(1)}(0,0)-M_2^{(1)}(0,0). \tag{4.23}$$

In either way, one finds

$$\mu^{(1)}=\frac{1}{2}\int\frac{d^3p}{(2\pi)^3}(\lambda_p-1)\frac{1}{p^2}$$

$$=-3.0349\times10^{-2}, \tag{4.24}$$

where λ_p is given by (4.21).

The integrals (4.20) are well defined and have been evaluated numerically for 20 values of k below the cutoff momentum $k=2$. The results are shown in Fig. 11. For small k, $\omega_k^2-\omega_{pl}^2$ is found to be proportional to k^2 (see Fig. 12). We find that

$$\lim_{k\to0}(\omega_k^2-\omega_{pl}^2)/k^2=-9.359\times10^{-3}\,g. \tag{4.25}$$

The quantity c^2, defined by (3.12), is, to order g,

$$c^2=n(d\mu/dn)=n(d/dn)\mu^{(1)}g\omega_{pl}$$

$$=\tfrac{1}{4}\mu^{(1)}g$$

$$=-7.587\times10^{-3}g. \tag{4.26}$$

We see that the inequality (3.12) is satisfied.

V. DISCUSSION

In the above analysis we have shown that a dielectric-constant formulation is quite effective in treating a charged Bose system. In fact, the difficulty due to the interaction at small-momentum transfers never appears. In contrast to the case of an electron gas, the 1-ring diagrams in Fig. 10 are *not* equivalent to a random-phase approximation, in which only Fig. 10(c) would survive. Thus, if one introduced the Bohm-Pines plasmon coordinates and made a random-phase approximation,[8] one would get incorrect results.

The second-order correction to the dispersion curve is enormously more complicated. Since there have been no experimental data on a high-density charged Bose system at zero temperature, we feel that the calculation to the second order would not be worthwhile.

ACKNOWLEDGMENT

We would like to thank Professor Keith A. Brueckner for suggesting the problem and for many helpful discussions.

[8] W. S. Chow, S. C. Lo, and K. W. Wong, Nuovo Cimento **43**, 316 (1966).